

Special Article - Cloth Texture

Ball-Milling Graphite Used for Synthesis of Biocompatible Blue Luminescent Graphene Quantum Dots

Zhou J^{1*}, Dong Y², Ma Y¹ and Zhang T³¹School of Electromechanic Engineering, Qingdao University, Qingdao 266071, China²School of Chemistry and Chemical Engineering, Qingdao University, Qingdao 266071, China³Professor, Schoolmaster, Shandong University of Technology, Zibo 255000, China

*Corresponding author: Jian Zhou, School of Electromechanic Engineering, Qingdao University, Qingdao 266071, China

Received: July 21, 2021; Accepted: August 17, 2021;

Published: August 24, 2021

Abstract

Graphene Quantum Dots (GQDs) have been prepared by oxidation-hydrothermal reaction, using ball-milling graphite as the starting materials. The prepared GQDs are endowed with excellent luminescence properties, with the optimum emission of 320nm. Blue photoluminescence emitted from the GQDs under ultraviolet light. The GQDs are ~3nm in width and 0.5~2 nm in thickness, revealed by high-resolution transmission electron microscopy and atomic force microscopy. In addition, Fourier transform infrared spectrum evidences the existence of carbonyl and hydroxyl groups, meaning GQDs can be dispersed in water easily and used in cellar imaging, and blue area inside L929 cells were clearly observed under the fluorescence microscope. Both low price of raw material and simple prepared method contribute to the high quality GQDs widespread application in future.

Keywords: Ball-milling graphite; Graphene quantum dots; Cellar imaging; Fluorescence; Biocompatibility

Introduction

In 2010, Geim and Novoselov were awarded the Nobel Prize in Physics for their work on graphene. Then the graphene was regarded as one of the most promising 2D carbon materials, and attracted widely investigation in terms of its formation, characteristics and applications. It is found that graphene has electron mobility that exceeds $15000\text{cm}^2\text{V}^{-1}\text{s}^{-1}$ at room temperature, extremely low electrical resistance ($10^{-6}\Omega\cdot\text{cm}$), high transparency (absorbing only 2.3% of light), and excellent thermal conductivity ($5300\text{Wm}^{-1}\text{K}^{-1}$) [1]. Therefore, they are treated as promising building blocks for high quality nanodevices owing to their superior thermal, electronic, and mechanical properties as well as their chemical inertness [2-6]. However, graphene prepared by reduction of exfoliated Graphene Oxide (GO) [2], solvothermal synthesis [7], and micromechanical cleavage [8], are generally not suitable for their direct application in nanodevices because of the large size, which are usually several hundred nanometers. Therefore, it is a highly desirable to design and develop nanometer-sized graphene pieces to meet the challenges, and Graphene Quantum Dots (GQDs) begin to be widespread concerned in research circles.

The unique optical properties of GQDs make them very promising as fluorescent probes in biomedical application and have thus attracted substantial research attention. Quantum dots are composed of a small number of atoms. Smaller size of such material limits the movement of electrons, resulting in a phenomenon known as the Quantum Confinement Effect (QCE). Based on band-gap theory, the more decreasing graphene size, the QCE more apparent [9-11]. In addition to the QCE, the zigzag and armchair edges of GQDs also have an important effect on the material properties. All these factors lead to GQDs' high biocompatibility, low toxicity,

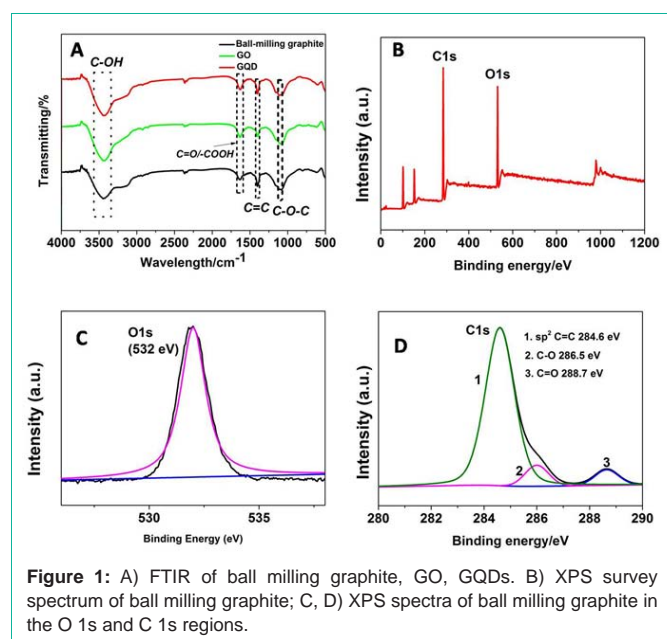
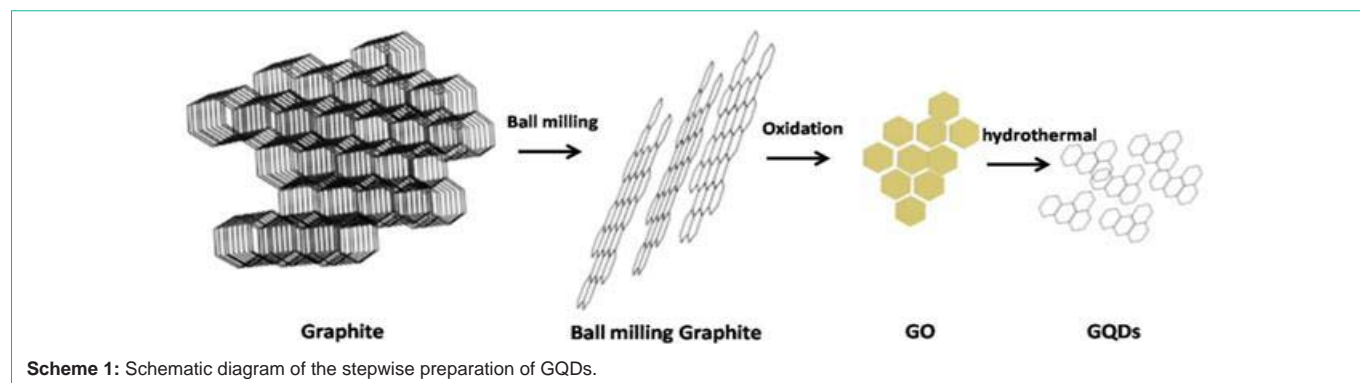
and photoluminescence, making GQDs available in biomedical applications, such as bioimaging [12], drug delivery [13], and biosensors [14]. Two methods have been developed for synthesis of GQDs including top-down synthesis and bottom-up synthesis, such as the hydrothermal approach [15] and chemical carbon nanofiber cutting [16], where a large graphene sheet is cut into small GQDs. With bottom-up methods, a series of chemical reactions are the key to synthesize GQDs, (solution chemistry) [17,18]. And, most "top-down" methods, such as electron beam lithography [19] require special equipment, complex procedures, low yield, critical synthesis conditions, thus further searching for new route to synthesize GQDs is of great interest.

GQDs with blue or green photoluminescence have been prepared by cutting graphene or other carbon sources (e.g. nanotubes, carbon fibers, C60) [20-23], including carving graphite crystallites using high-resolution electronbeam lithography [19], cutting GO *via* hydrothermal [15,22], reoxidation [24], or electrochemical routes [20], chemical oxidation treating carbon fibers and carbon black [25], cage opening the fullerene on ruthenium surfaces [23]. However, these methods still demonstrate tedious processing procedures and high-cost that it is urgent to find economic carbon sources with easy process to achieve the preparation of GQDs effectively.

Here, we use economic ball milling graphite as starting material, and oxidation-hydrothermal reaction to get high quality GQDs as shown in Scheme 1. Compared with others, the hydrothermal time can be reduced to 3h. And the resulting GQDs can be used in cell imaging. Both low price of raw material and simple prepared method will more contribute to the GQDs widespread application.

Results and Discussion

The starting material was ball-milling graphite processed in the



ball mill. A typical transmission electron microscopy (TEM) image of the ball milling graphite was shown in Figure S1, and its size was around 1 μm . Oxygen-containing functional groups, including C=O/COOH, -OH, and C-O-C were evidenced by FTIR spectrum (Figure 1A). Figure 2B shows the XPS survey spectrum of the ball milling graphite, indicating the presence of C and O elements. XPS spectrum in O 1s region (Figure 1C) shows a strong peak at 532 eV, which is typical for a hydroxyl group. Three peaks at 288.75 eV, 284.6 eV, 285.9 eV are presented in C 1s region, which are assigned to carboxyl groups (-COOH), the sp^2 carbon peak, hydroxyl (-OH), respectively (Figure 1D). After the oxidation of ball milling graphite into GO, the FTIR results (Figure 1A) show that the containing functional groups did not change. AFM image in Figure 2A reveals that its depth is among 0.5-1.2 nm. The lateral size of GO was around 15 nm as depicted in Figure 2B.

A series of more obvious changes take place after the hydrothermal treatment of the GO at 200°C for 10h. The resulting GQDs are characterized by FTIR, HRTEM, AFM and Raman. After the hydrothermal treatment, the strongest vibrational absorption band of C=O/COOH at 1650 cm^{-1} didn't change and the vibration band of epoxy groups at 1052 cm^{-1} shifted to 1108 cm^{-1} , which means the epoxy groups' disappearing (Figure 1A).

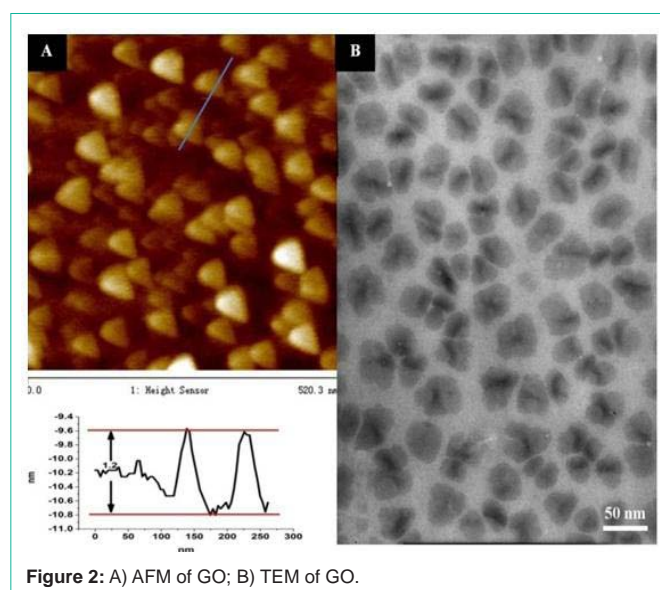


Figure 3 shows typical HRTEM of the GQDs. Their diameters are mainly around 4 nm and its high ordered graphite lattice were clearly observed. In Figure S2, the GQDs' AFM image, associating topographic heights are mostly between 0.5 and 2 nm. Figure S3 shows the Raman spectrum of GQDs. G band at 1596 cm^{-1} and D band at 1351 cm^{-1} were clearly observed with a large intensity ratio ID/IG of 1.18.

The most intriguing characteristic of GQDs is the phenomenon of a new PL behavior. The GQDs emit bright blue luminescence in neutral media as shown in Figure S4. The UV result in Figure 4A indicates that GQDs have the strong absorption at 430 nm, at the optical excitation of 320 nm. Like most luminescent carbon nanoparticles, the GQDs also exhibit an excitation-dependent PL behavior. When the excitation wavelength is changed from 290 to 360 nm, the PL peak did not show shifts, but its intensity decreases rapidly, when excitation wavelength was off 320 nm.

The hydrothermal time can be reduced to 3h to prepare GQDs. The PL of GQDs is shown in Figure 4B. When excitation is 320 nm, the strongest PL intensity appeared. And the excitation-dependent PL behavior is also similar to the GQDs prepared in 10h hydrothermal. The preparation efficiency of GQDs was greatly enhanced *via* shortening the hydrothermal time, which is beneficial for its broader application.

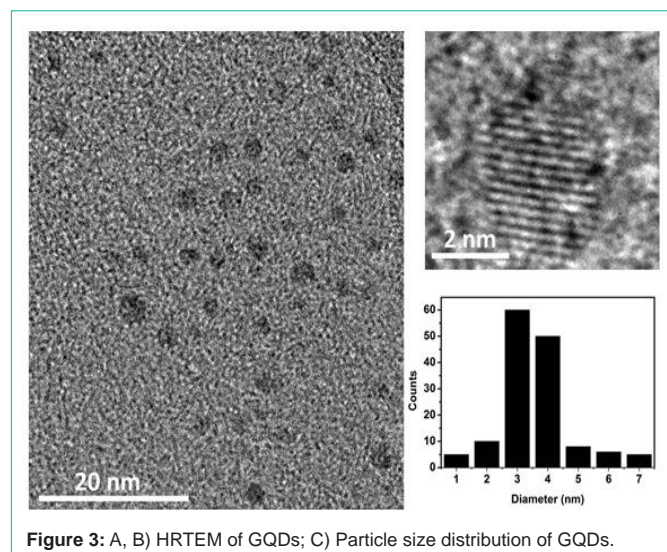


Figure 3: A, B) HRTEM of GQDs; C) Particle size distribution of GQDs.

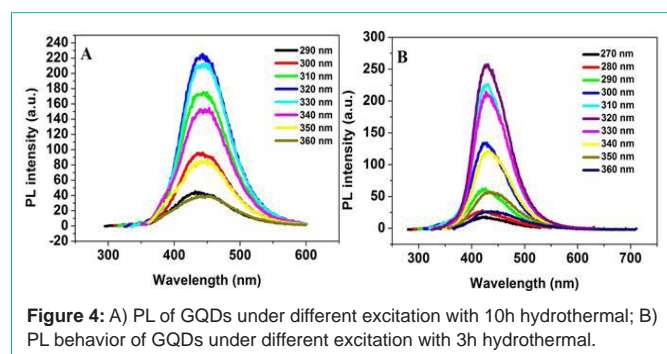


Figure 4: A) PL of GQDs under different excitation with 10h hydrothermal; B) PL behavior of GQDs under different excitation with 3h hydrothermal.

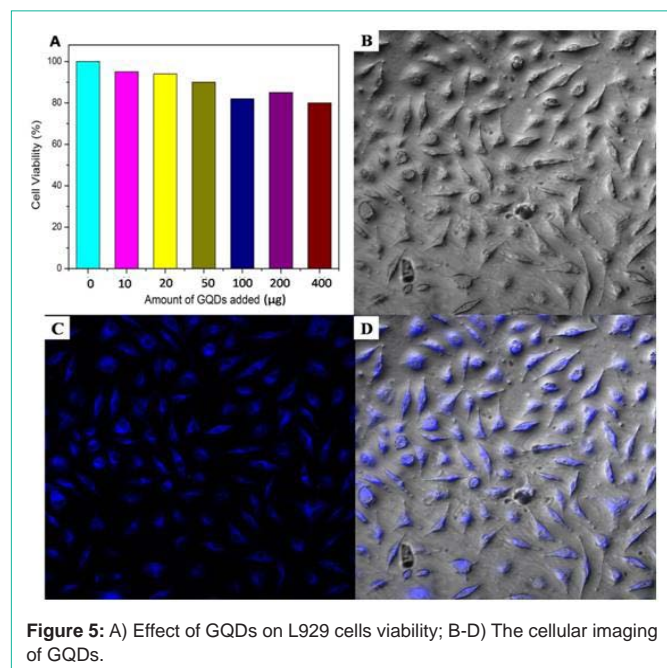


Figure 5: A) Effect of GQDs on L929 cells viability; B-D) The cellular imaging of GQDs.

Vitro cytotoxicity of GQDs was evaluated in L929 cells by MTT assay. Results suggest that even though the addition of 400µg GQDs, cell viability can still reach 80%, meaning GQDs low toxicity.

Fluorescence QDs are being paid great and wide attention in the fields of bio-imaging material of life science, because of their special fluorescence character. This prompts us to explore their potential application in cell labeling. From Figure 5B and 5C, we can see blue area inside L929 cells, indicating successful penetration of GQDs through cell membrane. Under continuous excitation over 15min, the PL brightness of GQDs was stable, indicating high photostability of GQDs. Besides biological imaging platforms, surface hydrophilic groups, biological compatibility, stable PL can also make GQDs be employed in surface modifications for further biomedical applications.

Conclusions

In conclusion, we have prepared GQDs using economic ball milling graphite with less hydrothermal time (3h). The prepared GQDs were endowed with excellent blue luminescence properties and used in culturing L929 cells and biological labeling, showing good photostability and low toxicity. Both low price of raw material and simple prepared method contribute to the high quality GQDs widespread application.

Acknowledgement

This work was supported by National Key R&D Program of China (2017YFB0102004).

References

- Geim AK and Novoselov KS. The rise of graphene. *Nat. Mater.* 2007; 6: 183-191.
- Li D, Muller MB, Gilje S, Kaner RB and Wallace GG. Processable aqueous dispersions of graphene nanosheets. *Nat. Nanotech.* 2008; 3: 101-105.
- Son Y-W, Cohen ML and Louie SG. Energy gaps in graphene nanoribbons. *Phy. Rev. Lett.* 2006; 97: 216803.
- Han MY, Özyilmaz B, Zhang Y and Kim P. Energy band-gap engineering of graphene nanoribbons. *Phy. Rev. Lett.* 2007; 98: 206805.
- Kosynkin DV, Higginbotham AL, Sinitskii A, Lomeda JR, Dimiev A and Price BK. Longitudinal unzipping of carbon nanotubes to form graphene nanoribbons. *Nature.* 2009; 458: 872-876.
- Li X, Wang X, Zhang L, Lee S and Dai H. Chemically derived, ultrasmooth graphene nanoribbon semiconductors. *Science.* 2008; 319: 1229-1232.
- Choucair M, Thordarson P, Stride JA. Gram-scale production of graphene based on solvothermal synthesis and sonication. *Nature Nanotech.* 2009; 4: 30-33.
- Novoselov KS, Geim AK, Morozov S, Jiang D, Zhang Y and Dubonos S. Electric field effect in atomically thin carbon films. *Science.* 2004; 306: 666-669.
- Zhang Z, Chang K and Peeters F. Tuning of energy levels and optical properties of graphene quantum dots. *Phys. Rev. B.* 2008; 77: 235411.
- Ritter KA and Lyding JW. The influence of edge structure on the electronic properties of graphene quantum dots and nanoribbons. *Nat. Mater.* 2009; 8: 235-242.
- Nair R, Blake P, Grigorenko A, Novoselov K, Booth T and Stauber T. Fine structure constant defines visual transparency of graphene. *Science.* 2008; 320: 1308-1308.
- Zhu S, Zhang J, Qiao C, Tang S, Li Y and Yuan W. Strongly green-photoluminescent graphene quantum dots for bio-imaging applications. *Chem. Commun.* 2011; 47: 6858-6860.
- Wang X, Sun X, Lao J, He H, Cheng T and Wang M. Multifunctional graphene quantum dots for simultaneous targeted cellular imaging and drug delivery. *Colloids Surf. B.* 2014; 122: 638-644.

14. Li X, Zhu S, Xu B, Ma K, Zhang J and Yang B. Self-assembled graphene quantum dots induced by cytochrome c: a novel biosensor for trypsin with remarkable fluorescence enhancement, *Nanoscale*. 2013; 5: 7776-7779.
15. Pan D, Zhang J, Li Z and Wu M. Hydrothermal route for cutting graphene sheets into blue-luminescent graphene quantum dots. *Adv. Mater.* 2010; 22: 734-738.
16. Peng J, Gao W, Gupta BK, Liu Z, Romero-Aburto R and Ge L. Graphene quantum dots derived from carbon fibers. *Nano Lett.* 2012; 12: 844-849.
17. Liu R, Wu D, Feng X and Müllen K. Bottom-up fabrication of photoluminescent graphene quantum dots with uniform morphology. *J. Am. Chem. Soc.* 2011; 133: 15221-15223.
18. Hamilton IP, Li, B, Yan X, Li L-S. Alignment of colloidal graphene quantum dots on polar surfaces. *Nano Lett.* 2011; 11: 1524-1529.
19. Ponomarenko L, Schedin F, Katsnelson M, Yang R, Hill E and Novoselov K. Chaotic Dirac billiard in graphene quantum dots. *Science*. 2008; 320: 356-358.
20. Li Y, Hu Y, Zhao Y, Shi G, Deng L and Hou Y. An electrochemical avenue to green-luminescent graphene quantum dots as potential electron-acceptors for photovoltaics. *Adv. Mater.* 2011; 23: 776-780.
21. Cheng H, Zhao Y, Fan Y, Xie X, Qu L and Shi G. Graphene-quantum-dot assembled nanotubes: A new platform for efficient raman enhancement. *ACS nano*. 2012; 6: 2237-2244.
22. Shen J, Zhu Y, Yang X, Zong J, Zhang J and Li C. One-pot hydrothermal synthesis of graphene quantum dots surface-passivated by polyethylene glycol and their photoelectric conversion under near infrared light. *New J. Chem.* 2012; 36: 97-101.
23. Lu J, Yeo PS, Gan CK, Wu P and Loh KP. Transforming C60 molecules into graphene quantum dots. *Nature Nanotech.* 2011; 6: 247-252.
24. Shen J, Zhu Y, Chen C, Yang X and Li C. Facile preparation and up conversion luminescence of graphene quantum dots. *Chem. Commun.* 2011; 47: 2580-2582.
25. Dong Y, Chen C, Zheng X, Gao L, Cui Z and Yang H. One-step and high yield simultaneous preparation of single-and multi-layer graphene quantum dots from CX-72 carbon black. *J. Mater. Chem.* 2012; 22: 8764-8766.